# Anisotropic electronic structure of orthorhombic RbC$_{60}$: A high-field ESR investigation

J. Rahmer,[1] A. Grupp,[1] M. Mehring,[1] J. Hone,[2] and A. Zettl[2]

[1]*2. Physikalisches Institut, Universität Stuttgart, Pfaffenwaldring 57, 70550 Stuttgart, Germany*

[2]*Department of Physics, University of California at Berkeley, and Materials Sciences Division, Lawrence Berkeley Laboratory, Berkeley, California 94720*

(Received 8 November 2000; published 7 February 2001)

The full anisotropy of the electronic $g$ tensor of a RbC$_{60}$ single crystal was determined by applying high-field ESR. The principal values of the $g$ tensor $g_{xx} = 2.0014$, $g_{yy} = 2.0012$, and $g_{zz} = 2.0019$ reflect the orthorhombic symmetry and 3D nature of this polymeric phase.

RbC$_{60}$ and CsC$_{60}$ belong to the class of fullerides with the largest number of stable and metastable phases. Among the different phases the polymeric orthorhombic phase, which forms at about 350 K when lowering the temperature from the high-temperature cubic phase, attracted most attention. The ground state of this phase below the metal-insulator transition around 50 K is still under debate. The polymer bonds formed by a 2+2 cycloaddition (two $sp^3$ bonds) result in an unusually short spacing of the fullerene molecules along the $a$ axis of the orthorhombic unit cell, which has led to the proposal of quasi-one-dimensional conductivity and a corresponding transition to a low-temperature spin-density wave (SDW) state[1] as in the Bechgaard salts like (TMTSF)$_2$PF$_6$.[2] This conjecture was supported by the observation of drastic ESR line broadening below the metal-insulator transition, which was interpreted as antiferromagnetic resonance (AFMR) being the typical fingerprint of a SDW, by Jánossy *et al.*[3] Since only powder samples were investigated up to then, the characteristic features of AFMR were only partially resolved. Others therefore issued a note of care concerning the interpretation of the ESR data.[4] If one assumes the AFMR interpretation to be correct it is still an open question whether the low-temperature phase is an SDW or 3D antiferromagnetic (AFM) state.

Settling this open question depends very much on the dimensionality or nesting properties of the metallic phase. Chauvet *et al.*[1] proposed a low-dimensional metallic state which may suggest itself due to the polymeric structure and more importantly by comparing the ESR linewidth with the cubic fulleride Rb$_3$C$_{60}$. Considering the same spin-orbit interaction for both metals the 3D metal is expected to show a much broader ESR line as compared with the 1D metal according to the Elliott theory.[5] The much narrower ESR linewidth observed in orthorhombic RbC$_{60}$ seems to justify this conjecture.

In this contribution we show that the $g$-tensor anisotropy (i) contributes to the ESR linewidth in powder samples in particular at high fields, and (ii) more importantly is consistent with a 3D metallic state. In order to separate $g$-tensor line shifts from dynamic broadening we performed a high-field (94 GHz) single-crystal ESR investigation.

The single-crystal samples were prepared by stoichiometricly doping C$_{60}$ crystals with rubidium and removing all unwanted phases by dissolving the crystal in toluene. A more detailed description of the procedure can be found in Ref. 6.

The dimensions of the crystals used by us are in the range from 0.3 to 0.5 mm. X-ray-diffraction measurements revealed that the crystals consist of a mosaic structure.[7] This does not affect our analysis too much, however, since the orientation dependence of the ESR lineshift is only of the sin/cos type. More serious is the appearance of different domains. These emerge when going from the fcc phase to the orthorhombic polymer phase. When passing through this phase transition there exists a total of six different orthogonal orientations of the domains. In the following we will deal with this situation.

RbC$_{60}$ single-crystal samples were investigated using ESR at X- and W-band frequencies, i.e., at 9 and 94 GHz. X-band measurements were performed using a standard Bruker spectrometer equipped with a TE$_{102}$ rectangular cavity. For the 94 GHz measurements a Bruker Elexsys 680 W-band spectrometer with a cylindrical cavity was used. We note that at W-band frequencies line shifts due to $g$ anisotropies are by a factor of 10 larger than at the X band.

ESR measurements performed at the X band showed a single Lorentzian line in the temperature range from about 40 K to room temperature (see inset of Fig. 1). Its width is related to the electronic dynamics which is governed by the conduction electron scattering.[5] At 50 K a linewidth of $\Delta B_{\text{FWHM}} = 0.352$ mT is observed with an isotropic $g$ factor $g_{\text{iso}} = 2.0015$. The linewidth increases strongly with temperature. Below the metal-insulator transition (40 K) the
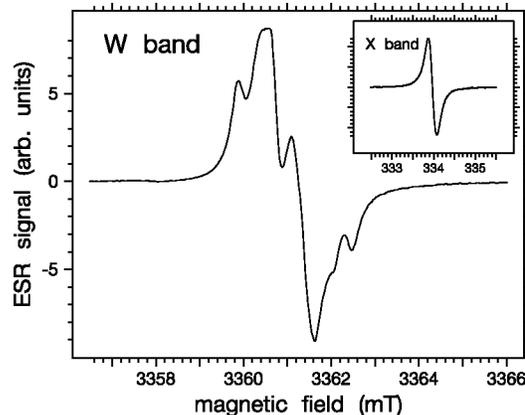


FIG. 1. Comparison of the resolved $g$ anisotropy line structure in the W band (94 GHz) with the unresolved Lorentzian line in the X band (9 GHz) (inset) at 50 K.
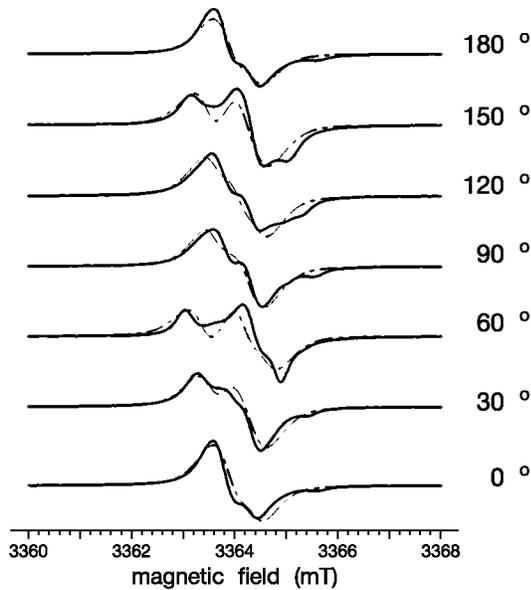
FIG. 2. Orientational dependence of the line structure at the W band at 50 K. The sample was rotated about an axis perpendicular to the field in steps of 30°. Dashed lines represent the spectra obtained from a genetic fitting procedure as described in the text.

TABLE I. $g$-tensor values and their standard deviation resulting from ten different simulations: the different tensor elements are defined as $g_{iso} = \frac{1}{3}(g_{xx} + g_{yy} + g_{zz})$, $\Delta g = (g_{zz} - g_{iso})$, and $\eta = (g_{xx} - g_{yy})/\Delta g$. $g_{iso}$ was determined in the X band by comparison with a standard; its error is the experimental accuracy.

| | $g$-tensor values | | |
|---|---|---|---|
| | $g_{iso}$ | $\Delta g$ | $\eta$ |
| Average | 2.0015 | 0.00038 | 0.61 |
| Error | 0.0001 | 0.00004 | 0.12 |
| | $g_{xx}$ | $g_{yy}$ | $g_{zz}$ |
| Average | 2.00143 | 2.00119 | 2.00188 |
| Error | 0.00013 | 0.00016 | 0.00014 |

linewidth increases again resulting in a minimal linewidth at around 60 K.

The W-band spectrum corresponds to a set of overlapping Lorentzian lines arising from the different unit cell orientations of the crystal with respect to the magnetic field. Rotation of the sample reveals a strong orientational dependence of the line pattern, as displayed in Fig. 2. The sample was rotated in steps of 30° to obtain the series of spectra. In order to determine the full $g$ tensor, which describes the electronic anisotropy of the unit cell, the single-crystal spectrum is analyzed for a number of different orientations (see Fig. 2). This is not a trivial task, because of the domain structure of the crystals.

All differently oriented domains are expected to have the same $g$ tensor. According to the orthorhombic structure we expect six different orientations of domains. Correspondingly our simulation uses a weighted sum of six different tensor orientations. In its local frame, the $g$ tensor is characterized by $g_{iso} = \frac{1}{3}(g_{xx} + g_{yy} + g_{zz})$, $\Delta g = (g_{zz} - g_{iso})$, $\eta = (g_{xx} - g_{yy})/\Delta g$. Since the weight of each of the domains is unknown we introduce it as a fitting parameter. For simplicity we assume the same orientation-independent ESR linewidth for all individual lines. Altogether, 13 parameters determine the spectrum: six weight factors, the linewidth, three parameters corresponding to the three principal values of the $g$ tensor, and three Euler angles describing the orientation of the crystal with respect to the magnetic field.

All seven spectra displayed in Fig. 2 were fitted at once. This was achieved with a simulation program written in C/C++ which calculates a set of single-crystal spectra using the Gamma library,[8] determines the standard deviation with respect to the set of experimental spectra and uses a genetic algorithm to minimize the errors by varying all parameters.

Several thousand steps are required to achieve a reasonable agreement between the simulation and the data. A typical example of a fit is represented by the dashed lines in Fig. 2. For the fit in Fig. 2 the relative weights $(1.00, 1.02, 0.19, 1.80, 2.06, 0.12)$ of the six domains were obtained.

To increase the confidence level of the fitting procedure, the genetic algorithm was started from random initial parameter sets several times. The resulting Euler angles vary strongly from one fit to the other, because there is a high degree of degeneracy among the different orientations for the domains with respect to the sample frame. Nevertheless the $g$-tensor values show only slight variations. Table I lists the average value of the parameters extracted from ten different runs of the simulation, together with the standard deviation for these ten sets.

From Fig. 2 it is obvious that the simulation does match the spectra pretty well although not completely. We believe this to be due to the fact that the sample is not a perfect single crystal, but contains small contributions from unoriented and disordered interdomain material. Nevertheless the standard error for the values found is rather small, so that within the limits of our model we are quite optimistic about the accuracy of the results. In conclusion we determined the nonaxial $g$ tensor for the orthorhombic polymer phase of $RbC_{60}$, with principal values $g_{xx} = 2.00143$, $g_{yy} = 2.00119$, and $g_{zz} = 2.00188$ corresponding to an isotropic $g$ factor of $g_{iso} = 2.0015$.

In what follows we will draw a connection between the $g$ tensor and the electronic structure. Band-structure calculations which include the calculation of the $g$ tensor are unfortunately not available. We must therefore resort to symmetry arguments. It follows from symmetry that the principal axes must correspond to the $a$, $b$, $c$ axes of the orthorhombic unit cell. Because of the domain structure of the sample we cannot determine the relation between the $g$-tensor principal axes $(x, y, z)$ and the $(a, b, c)$ crystal axes from the experimental data alone. We note, however, that the conduction electron spin-density distribution as determined from NMR data[9,10] has the polymer axis $(a)$ as its unique axis. We therefore conjecture that the same axis corresponds to the unique axis of the $g$ tensor ($z$ axis). The anisotropy in the plane perpendicular to the $a$ axis ($b, c$ or $x, y$ axes) is appreciable but much less than between the $z$ axis and the $x, y$

axes, consistent with the orthorhombic band structure as calculated by Erwin *et al.*[11]

In conclusion the $g$-tensor parameters are fully consistent with a 3D electronic structure of orthorhombic $RbC_{60}$. Moreover, comparing the deviation of the isotropic $g$ factor ($\delta g = 2.0023 - g_{iso}$) of $Rb_3C_{60}$ [$\sim 0.035$ at 50 K (Ref. 12)] with the one for $RbC_{60}$ (0.0008) and considering that the linewidth is proportional to $\delta g^2$ according to the Elliott mechanism, one expects a linewidth ratio of $\Delta B(Rb_3C_{60})/\Delta B(RbC_{60}) \approx 1900$. Comparing this to the linewidth ratio of the measured ESR signals, $\Delta B(Rb_3C_{60})/\Delta B(RbC_{60}) \approx 400$, using $\Delta B_{FWHM}(Rb_3C_{60})$

$\approx 140$ mT at 50 K from Ref. 12 and $\Delta B_{FWHM}(RbC_{60}) = 0.352$ mT from our X-band measurement, it becomes obvious that there is no need at all to interpret the ''narrow'' $RbC_{60}$ ESR line in terms of a quasi-one-dimensional metal. It should be noted that the 3D nature of the electronic state suggests an antiferromagntic ground state rather than an SDW ground state.

[1] O. Chauvet, G. Oszlányi, L. Forró, P. W. Stephens, M. Tegze, G. Faigel, and A. Jánossy, Phys. Rev. Lett. **72**, 2721 (1994).

[2] K. Mortensen, Y. Tomkiewicz, T. D. Schultz, and E. M. Engler, Phys. Rev. Lett. **46**, 1234 (1981).

[3] A. Jánossy, N. Nemes, T. Fehér, G. Oszlányi, G. Baumgartner, and L. Forró, Phys. Rev. Lett. **79**, 2718 (1997).

[4] M. Bennati, R. G. Griffin, S. Knorr, A. Grupp, and M. Mehring, Phys. Rev. B **58**, 15 603 (1998).

[5] R. J. Elliott, Phys. Rev. **96**, 266 (1954).

[6] J. Hone, M. S. Fuhrer, K. Khazeni, and A. Zettl, Phys. Rev. B **52**, R8700 (1995).

[7] P. Launois, R. Moret, J. Hone, and A. Zettl, Phys. Rev. Lett. **81**, 4420 (1998).

[8] S. A. Smith, T. O. Levante, B. H. Meier, and R. R. Ernst, J. Magn. Reson. **106a**, 75 (1994).

[9] T. M. de Swiet, J. L. Yarger, T. Wagberg, J. Hone, B. J. Gross, M. Tomaselli, J. J. Titman, A. Zettl, and M. Mehring, Phys. Rev. Lett. **84**, 717 (2000).

[10] M. Mehring, K. F. Thier, F. Rachdi, and T. de Swiet, Carbon **38**, 1625 (2000).

[11] S. C. Erwin, G. V. Krishna, and E. J. Mele, Phys. Rev. B **51**, R7345 (1995).

[12] P. Petit, J. Robert, T. Yildirim, and J. E. Fischer, Phys. Rev. B **54**, R3764 (1996).